

Optimization of the CMB-galaxy cross-correlation signal for studying the Integrated Sachs-Wolfe effect

Arthur Diniz Meirelles

Advisor: Edivaldo Moura Santos

Coadvisor: Ronaldo Carloto Batista

Institute of Physics
Universidade de São Paulo

15/08/2024



- 1 Theoretical Aspects
- 2 Optimized Galaxy Survey
- 3 Data Processing
- 4 Analysis and Results
- 5 Conclusions

1 Theoretical Aspects

2 Optimized Galaxy Survey

3 Data Processing

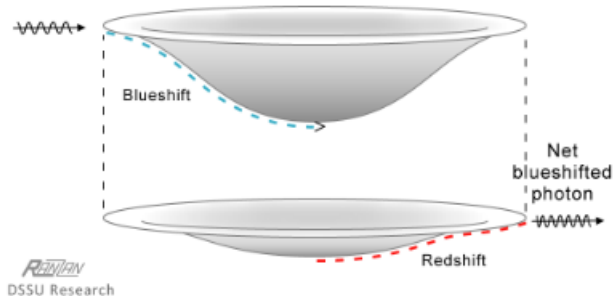
4 Analysis and Results

5 Conclusions

Introduction

- The integrated Sachs-Wolfe (ISW) effect occurs due to time changes in gravitational potentials;
- During periods of transition from or to matter-dominated eras of the Universe, potentials change more rapidly;
- Photons that enter gravity wells are affected by gravitational blueshift. After traveling across them during these transition periods, the redshift affecting the photon when it escapes that well does not match the previous blueshift, leaving either a net blueshift or redshift in the photon.

Introduction



Naturally, a statistical correlation between CMB temperature maps and gravitational potentials is expected.

Figure 2: Illustration of the ISW effect. In this case, the gravity wells flattened, leaving a net blueshift.

The Λ CDM Model

To build the theoretical framework used, it is assumed

- The Universe is homogeneous and isotropic at large scales;
- During its very early stages, it was very compact and energetic;
- An inflationary period is assumed;
- Aside from baryonic matter, radiation and neutrinos, the Universe is also composed of cold dark matter and a dark energy component described by a cosmological constant Λ ;

The homogeneous and isotropic background is first set up, and linear perturbations are added to it.

The Cosmic Microwave Background

The temperature of the Cosmic Microwave Background (CMB) can be expressed by

$$T(\mathbf{x}, \hat{\mathbf{p}}, t) = \bar{T}(t)[1 + \Theta(\mathbf{x}, \hat{\mathbf{p}}, t)]. \quad (1)$$

The temperature perturbation Θ can be expressed in Fourier space according to

$$\Theta(\hat{\mathbf{k}}, \mu) = \sum_{\ell=0}^{\infty} (2\ell + 1)(-i)^{\ell} \Theta_{\ell}(\hat{\mathbf{k}}) \mathcal{P}_{\ell}(\mu), \quad (2)$$

where

$$\Theta_{\ell} = \frac{1}{(-1)^{\ell}} \int_{-1}^1 \frac{\mathcal{P}_{\ell}(\mu) \Theta(\mu)}{2} d\mu, \quad \mu = \hat{\mathbf{k}} \cdot \hat{\mathbf{p}}. \quad (3)$$

Analytical Approximation

Working with first-order equations and the tightly coupled limit, and assuming recombination to be an instantaneous process happening at conformal time $\eta = \eta_*$, we can obtain the following analytical solution for the CMB temperature perturbations

$$\begin{aligned} \Theta_\ell(k, \eta_0) \approx & [\Theta_0(k, \eta_*) + \Psi(k, \eta_*)] j_\ell[k(\eta_0 - \eta_*)] \\ & + i v_b(k, \eta_*) \left\{ j_\ell[k(\eta_0 - \eta_*)] - (\ell + 1) \frac{j_\ell[k(\eta_0 - \eta_*)]}{k(\eta_0 - \eta_*)} \right\} \\ & + \int_0^{\eta_0} d\eta e^{-\tau} [\Psi'(k, \eta) - \Phi'(k, \eta)] j_\ell[k(\eta_0 - \eta)]. \end{aligned} \quad (4)$$

Here, the third term in the equation describes the Integrated Sachs-Wolfe effect.

Correlation Functions

To calculate the CMB autocorrelation function C_ℓ^{tt} , we expand Θ in spherical harmonics

$$\Theta(\mathbf{x}, \hat{\mathbf{p}}, t) = \sum_{\ell=1}^{\ell_{\max}} \sum_{m=-\ell}^{\ell} a_{\ell m}(\mathbf{x}, t) Y_{\ell m}(\hat{\mathbf{p}}), \quad (5)$$

and calculate the autocorrelation between the $a_{\ell m}$ terms:

$$\langle a_{\ell m} a_{\ell' m'}^* \rangle = \delta_{\ell \ell'} \delta_{m m'} C_\ell^{tt} \quad (6)$$

Other autocorrelation spectra C_ℓ^{xx} follow the same process. It is common to use

$D_\ell^{XX} = \frac{\ell(\ell+1)}{2\pi} C_\ell^{xx}$ for some spectra for better visualization.

Cosmic Variance

The low number of $a_{\ell m}$ coefficients for lower multipoles ℓ leads to a high uncertainty in this region called cosmic variance

$$\left(\frac{\Delta C_{\ell}^{XX}}{C_{\ell}^{XX}} \right)_{CV} = \sqrt{\frac{2}{2\ell + 1}} \quad (7)$$

Planck 2018

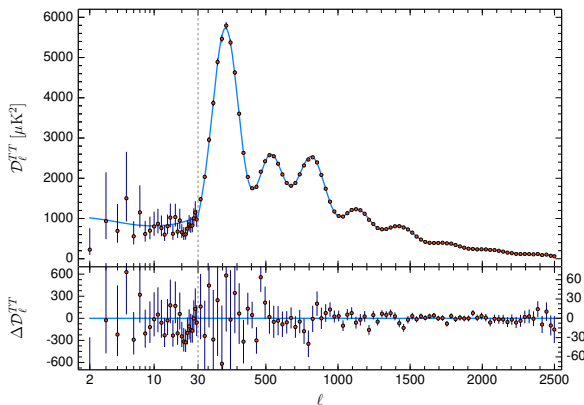


Figure 3: Planck 2018 CMB temperature power spectrum.

Parameter	Best-fit
$\Omega_b h^2$	0.02237 ± 0.00015
$\Omega_c h^2$	0.1200 ± 0.0012
$100\Theta_{MC}$	1.04092 ± 0.00031
τ	0.0544 ± 0.0073
$\ln(10^{10} A_s)$	3.044 ± 0.014
n_s	0.9649 ± 0.042
Ω_m	0.3153 ± 0.0073
H_0	$67.36 \pm 0.54 \text{ km/s/Mpc}$
σ_8	0.8111 ± 0.0060

Table 1: Best fit values of cosmological parameters reported in Planck 2018 results.

The Matter Power Spectrum

To calculate a cross-correlation function, we need the 3D matter power spectrum $P(k, z)$, defined by

$$\langle \delta(\mathbf{k}, z) \delta^*(\mathbf{k}', z) \rangle = (2\pi)^3 P(k, z) \delta_D(\mathbf{k} - \mathbf{k}') \quad (8)$$

The Matter Power Spectrum

Throughout this project, we have used CAMB's implementation of the HALOFIT model to calculate the matter power spectrum.

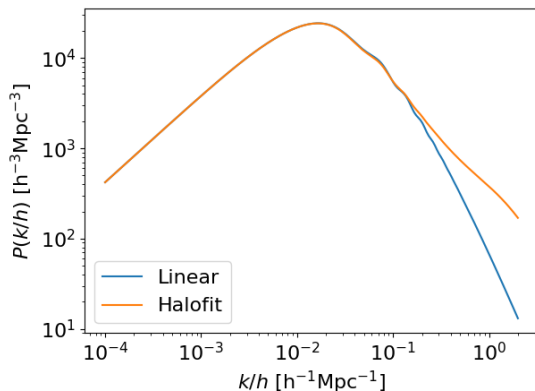


Figure 4: Matter power spectrum calculated using both a linear approximation and the so-called HALOFIT model.

The Cross-correlation Spectrum

To trace the matter density anisotropies, we used galaxy contrast maps, which can be calculated using

$$\delta_g(\mathbf{k}) = \frac{\rho_g(\mathbf{k}) - \bar{\rho}_g}{\bar{\rho}_g} \quad (9)$$

It is assumed that $\delta_g = b_g \delta$, where b_g , which we assume to be a slowly varying function of redshift.

The cross-correlation function C_ℓ^{tg} can then be calculated with

$$\langle a_{\ell m}^t a_{\ell' m'}^g \rangle = C_\ell^{tg} \delta_{\ell \ell'} \delta_{mm'} \quad (10)$$

Analytical Formula

Given fields x and y , representing either the ISW contribution to the CMB temperature ($x, y = t$) or the galaxy contrast ($x, y = g$), we can calculate the associated auto- or cross-correlation spectra using

$$C_{\ell}^{xy} = \frac{2}{\pi} \int dk k^2 W_{\ell}^x(k) W_{\ell}^y(k) P(k), \quad (11)$$

with

$$W_{\ell}^t = -3\Omega_m \left(\frac{H_0}{k} \right)^2 \int dz \frac{d[(1+z)D(z)]}{dz} j_{\ell}[k\chi(z)] \quad (12)$$

$$W_{\ell}^g = \int dz b_g(z) \frac{dN}{dz} D(z) j_{\ell}[k\chi(z)] \quad (13)$$

ISW Contribution: Temperature Autocorrelation

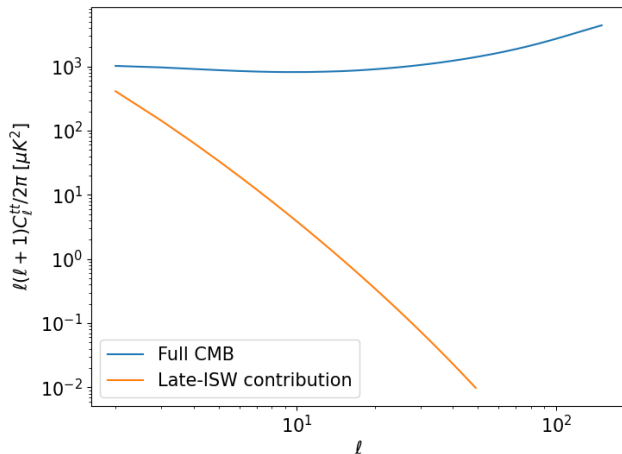


Figure 5: CMB autocorrelation comparison between full spectrum and ISW contribution.

ISW Contribution: Galaxy Autocorrelation and Cross-correlation

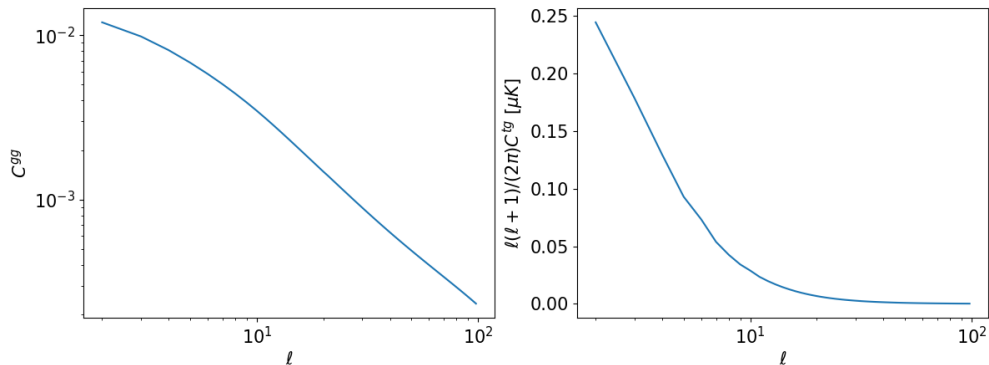


Figure 6: Galaxy autocorrelation spectrum (left) and late-ISW contribution to the galaxy-CMB cross-correlation (right).

- ① Theoretical Aspects
- ② Optimized Galaxy Survey**
- ③ Data Processing
- ④ Analysis and Results
- ⑤ Conclusions

Selection Function Parametrization

The function $\frac{dN}{dz}$ in equation (13) is called the selection function. We are assuming its parametrization to be

$$\frac{dN}{dz}(z|\lambda, \beta, z_0) dz = \frac{\beta}{\Gamma(\lambda)} \left(\frac{z}{z_0}\right)^{\beta\lambda-1} \exp\left[-\left(\frac{z}{z_0}\right)^\beta\right] d\left(\frac{z}{z_0}\right) \quad (14)$$

We have explored how to maximize the cross-correlation signal using an idealized selection function.

2MASS Bands Comparison

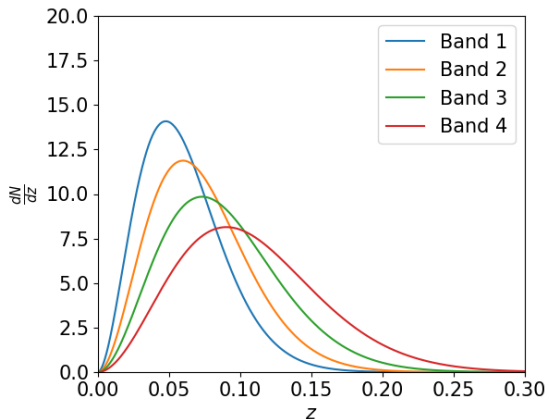


Figure 7: Selection function calculated for the 4 bands of the 2MASS catalog.

Band	z_0	β	λ
1	0.043	1.825	1.524
2	0.054	1.800	1.600
3	0.067	1.765	1.636
4	0.084	1.723	1.684

Table 2: Parameter values for the 4 bands of the 2MASS catalog.

Exploring the Parameter Space

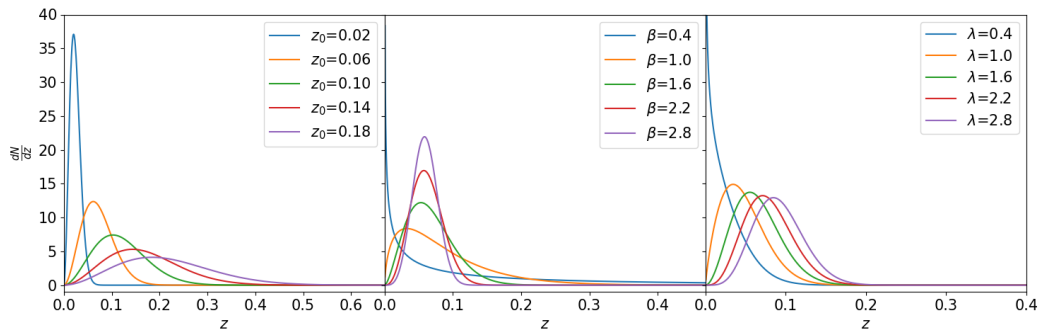


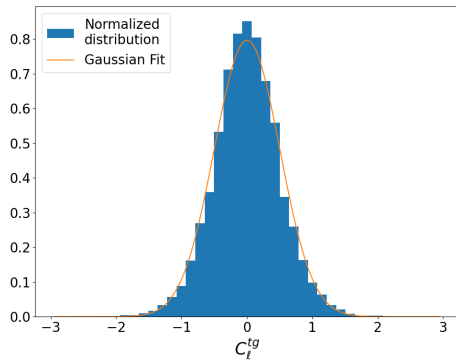
Figure 8: Selection function calculated for various parameter values.

Null Hypothesis

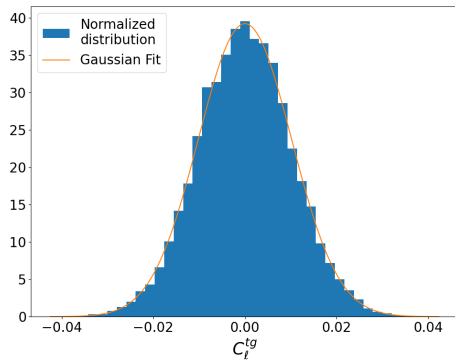
For the process of finding a galaxy survey with an idealized selection function, we first needed an estimation for the probability of C_ℓ^{tg} being 0, which would be our null hypothesis. The following process was used:

- Synthesize multiple uncorrelated CMB temperature and galaxy contrast maps using HEALPix;
- Calculate the cross-correlation C_ℓ^{tg} for each pair of uncorrelated maps at each multipole;
- For each multipole ℓ , a histogram of C_ℓ^{tg} was produced;
- Each histogram was fit with Gaussian distributions with average $\mu = \mu_\ell \approx 0$ and $\sigma^2 = \sigma_\ell^2$.

Synthesized Maps' Histograms



(a) $\ell = 4$



(b) $\ell = 30$

Figure 9: Distribution of cross-correlation values on different multipoles for 10^4 maps synthesized with null cross-correlation.

Null Hypothesis

For f_ℓ corresponding to the Gaussian fit made for the multipole ℓ

$$f_\ell(C_\ell^{tg}) = \frac{1}{\sqrt{2\pi\sigma_\ell^2}} \exp \left[-\frac{1}{2} \left(\frac{C_\ell^{tg} - \mu_\ell}{\sigma_\ell} \right)^2 \right], \quad (15)$$

we have defined the null hypothesis probability distribution to be

$$P_{\text{null}} = \prod_{\ell=2}^{\ell_{\text{max}}} f_\ell(C_\ell^{tg}) \quad (16)$$

Exploring the Parameter Space

For various points (β, z_0, λ) in the parameter space, we have calculated the ratio $P_{\text{null}}(\beta, z_0, \lambda) / P_{\text{null}}^{\text{2MASS}}$ and produced the heat maps in Figure 10.

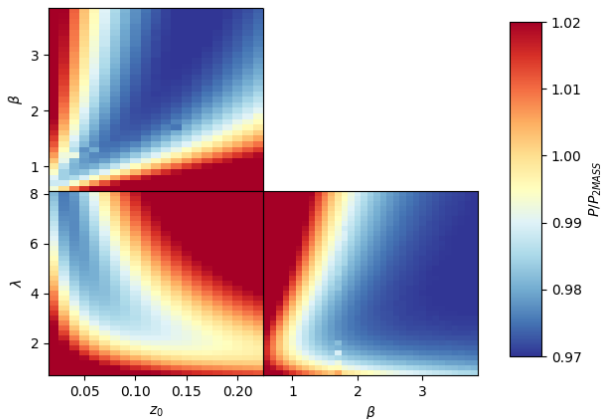


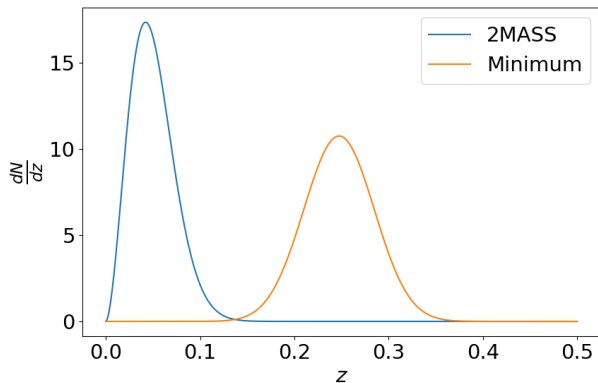
Figure 10: Heat maps used to explore the parameter space.

Minimizer

The heat maps provided initial points to run an algorithm that minimizes $P_{\text{null}}(z_0, \beta, \lambda)$. The point found that minimizes the null hypothesis probability in that region of the parameter space was

$$(\beta, z_0, \lambda) = (3.088, 0.1508, 4.9401) \quad (17)$$

Properties of the Minimum



The selection function found is deeper than that of 2MASS band 1, but does not favor galaxies at the expected value of $z^* = 0.63$, the estimated redshift at which the accelerated expansion started.

Figure 11: Selection functions comparison.

Properties of the Minimum

The selection function found reduces the maximum value of the cross-correlation function, but its peak is at higher redshifts ($\ell \approx 10$), reducing the influence of cosmic variance in the signal.

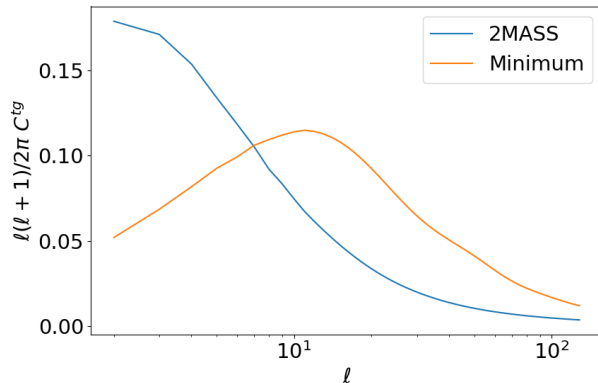


Figure 12: Theoretical cross-correlation spectrum comparison.

Discussion

- The ratio $P_{\text{null}}(z_0, \beta, \lambda) / P_{\text{null}}^{2\text{MASS}} = 0.971$ for the minimum;
- Despite the small statistical gain, this optimal selection function yields reasonably better results for constraints on Ω_m , as will be discussed;

- 1 Theoretical Aspects
- 2 Optimized Galaxy Survey
- 3 Data Processing**
- 4 Analysis and Results
- 5 Conclusions

WMAP Data

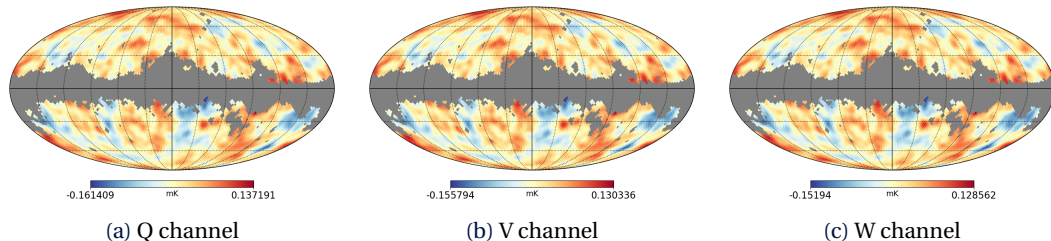
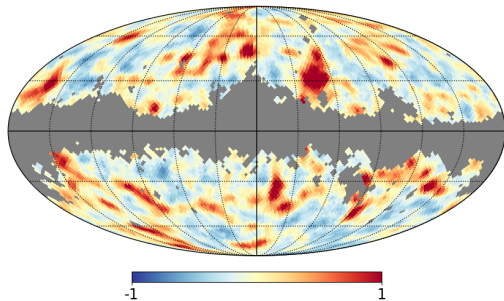
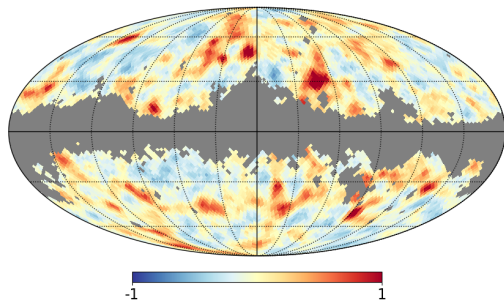


Figure 13: Mollweide projection of three (Q, V, W) WMAP9 CMB temperature (in mK) maps in galactic coordinates with an $f_{\text{sky}} = 0.70$ mask applied

2MASS Catalog



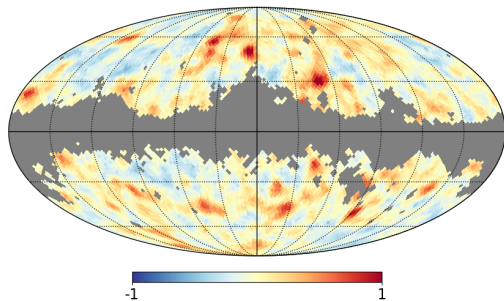
(a) Band 1



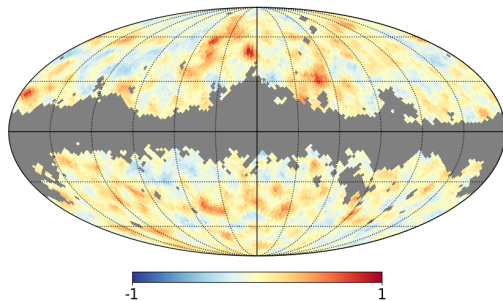
(b) Band 2

Figure 14: Mollweide projection of the 2MASS-XSC galaxy contrast maps in galactic coordinates with the combined 2MASS+WMAP mask applied ($f_{sky} = 0.70$).

2MASS Catalog



(a) Band 3



(b) Band 4

Figure 15: Mollweide projection of the 2MASS-XSC galaxy contrast maps in galactic coordinates with the combined 2MASS+WMAP mask applied ($f_{sky} = 0.70$).

Correlation Spectra Estimator

To estimate the correlation spectra that describe the pixelized maps d with primordial signal s and noise n (with \mathbf{S} and \mathbf{N} being the corresponding covariance matrices), we need to be able to sample from $P(\mathbf{C}|\mathbf{s}, d)$ and $P(\mathbf{s}|\mathbf{C}, d)$ with $\mathbf{C} = \mathbf{S} + \mathbf{N}$. Then we iterate

$$\mathbf{s}^{i+1} \leftarrow P(\mathbf{s}|\mathbf{C}, d) \quad (18)$$

$$\mathbf{C}^{i+1} \leftarrow P(\mathbf{C}|\mathbf{s}, d), \quad (19)$$

to obtain a sample of $\{(\mathbf{s}^i, \mathbf{C}^i)\}$.

The Blackwell-Rao Estimator

We can then use the Blackwell-Rao estimator to obtain an approximation for $P(C_\ell|\mathbf{d})$

$$P(C_\ell|\mathbf{d}) \approx \frac{1}{N_G} \sum_{i=1}^{N_G} P(C_\ell|\sigma_\ell^i), \quad (20)$$

where

$$\sigma_\ell^i = \frac{1}{2\ell+1} \sum_{m=-\ell}^{\ell} \mathbf{s}_{\ell m} \mathbf{s}_{\ell m}^\dagger. \quad (21)$$

We then maximize the probability $P(C_\ell|\mathbf{d})$ to obtain the best-fit C_ℓ .

Correlation Spectra Obtained

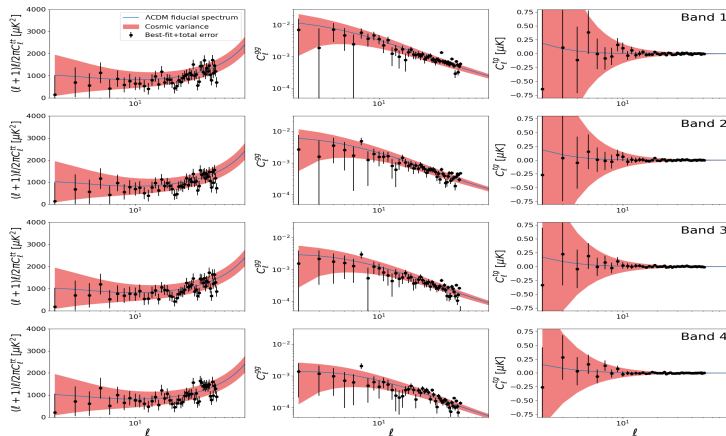


Figure 16: Comparison between theoretical correlation spectra and the ones estimated from WMAP and 2MASS.

- ① Theoretical Aspects
- ② Optimized Galaxy Survey
- ③ Data Processing
- ④ Analysis and Results**
- ⑤ Conclusions

Likelihood Profiling

To analyze the data, we have opted to profile the likelihood functions applied to Ω_m . The likelihood of each point in the spectrum was assumed to be Gaussian

$$\mathcal{L}(C_{\ell, \text{theo}}^{xy} | C_{\ell, \text{data}}^{xy}) = \frac{1}{\sigma_\ell \sqrt{2\pi}} \exp \left[-\frac{1}{2} \left(\frac{C_{\ell, \text{data}}^{xy} - C_{\ell, \text{theo}}^{xy}}{\sigma_\ell} \right)^2 \right]. \quad (22)$$

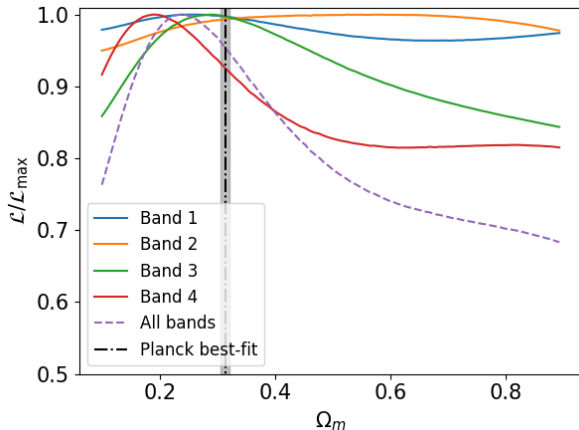
We are varying only Ω_m , so $C_{\ell, \text{theo}}^{xy}$ is a functions of only Ω_m . The likelihood of a full spectrum is

$$\mathcal{L}(\Omega_m | C_{\text{data}}^{xy}) = \prod_{\ell=2}^{\ell_{\max}} \mathcal{L}(C_{\ell, \text{theo}}^{xy} | C_{\ell, \text{data}}^{xy}). \quad (23)$$

The $C^{tg} + C^{gg}$ joint-likelihood is

$$\mathcal{L}(\Omega_m | C_{\text{data}}^{tg}, C_{\text{data}}^{gg}) = \mathcal{L}(\Omega_m | C_{\text{data}}^{tg}) \mathcal{L}(\Omega_m | C_{\text{data}}^{gg}). \quad (24)$$

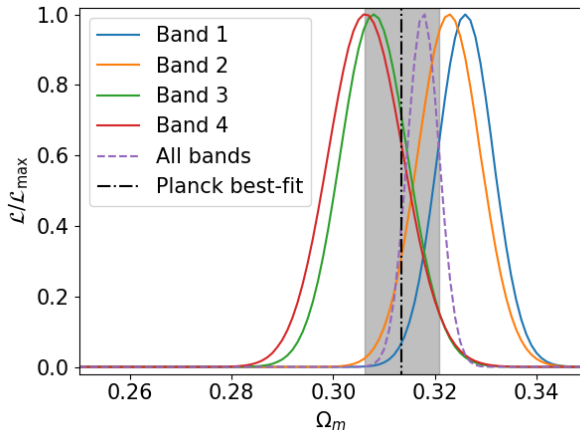
Results for 2MASS



- All curves are compatible with Planck;
- Not much constraining power on Ω_m ;
- Bands 3 and 4 – which have the deepest selection functions – have the most constraining power amongst all 4.

Figure 17: C^{tg} only likelihood profiles.

Results for 2MASS



- All likelihoods are compatible with Planck;
- Very high constraining power on Ω_m when C^{gg} is introduced, comparable to Planck's;
- No significant difference in constraining power between each band.

Figure 18: Joint likelihood profiles

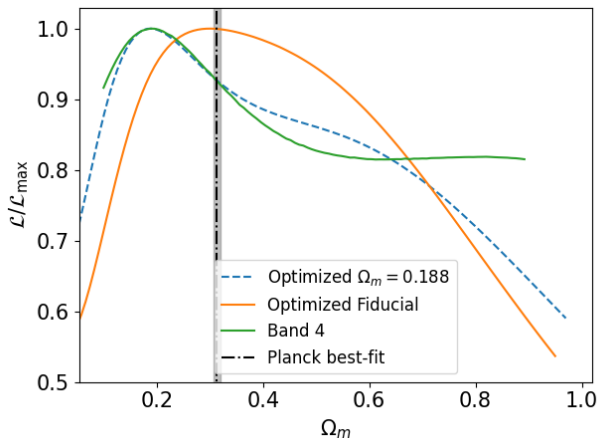
Forecast for the Optimized Band

To estimate the behavior of a survey that follows our idealized selection function in this analysis, we have produced two synthetic cross-correlation spectra using that selection function. Both use the Λ CDM model with Planck's best-fit parameters, only differing in Ω_m :

- One of the datasets was produced using Planck's best-fit of $\Omega_m = 0.3153$;
- The other dataset was produced using $\Omega_m = 0.188$, the value that maximizes the likelihood of band 4 for the C^{tg} only likelihood.

Band 4's errors were used as estimated for both synthetic datasets.

Forecast for the Optimized Band



- Constraining power still low;
- Reasonable improvement in the constraining power.

Figure 19: Optimized band C^{tg} only profile.

Discussion

- The optimized band being deeper than 2MASS means errors on the spectra should be higher, meaning the errors used are underestimated, which indicates the constraints could be better for a real survey following our optimized selection function;
- The optimized band was not found by optimizing the Ω_m constraints, but rejecting the null cross-correlation hypothesis. This null hypothesis leads to $\Omega_m = 1$, and the fast decrease in likelihood for higher Ω_m is noticeable;
- A similar work ... ?

- 1 Theoretical Aspects
- 2 Optimized Galaxy Survey
- 3 Data Processing
- 4 Analysis and Results
- 5 Conclusions**

Conclusions

- We have obtained the likelihood profiles for Ω_m obtained from cross-correlation data by studying the ISW effect;
- The constraints obtained using only C^{tg} were not strong, but can be used as a complement to other datasets for a combined analysis;
- In the 2MASS catalog, the 2 deepest bands – bands 3 and 4 – yielded better constraining power;

Conclusions

- An optimized band capable of maximizing the ISW signal was obtained, prioritizing galaxies at higher redshifts and increasing the cross-correlation signal in a region less affected by cosmic variance;
- The likelihoods obtained for artificial data calculated using the optimized band improved the constraints on Ω_m ;
- Combining different matter tracers leads to improved results overall.

Thank You

Extra Content

Discussão de Future prospects

Extra Content

More extras